Structural Fluctuations of Myoglobin from Normal-Modes, Mössbauer, Raman, and Absorption Spectroscopy

B. Melchers,* E. W. Knapp,* F. Parak,‡ L. Cordone,§ A. Cupane,§ and M. Leone§
*Freie Universität Berlin, Fachbereich Chemie, Institut für Kristallographie, 14195 Berlin, Germany; ‡Technische Universität, München Fakultät für Physik, 85748 Garching b. München, Germany; and §Istituto Di Fisica, Università di Palermo, and Istituto Nazionale Fisica della Materia Via Archirafi 36, 90123 Palermo, Italy

ABSTRACT A normal-mode analysis of carbon monoxymyoglobin (MbCO) and deoxymyoglobin (Mb) with 170 water molecules is performed for ^{54}Fe and ^{57}Fe. A projection is defined that extracts iron out-of-plane vibrational modes and is used to calculate spectra that can be compared with those from resonance Raman scattering. The calculated spectra and the isotopic shift ^{57}Fe versus ^{54}Fe agree with the experimental data. At low temperatures the average mean square fluctuations (MSFs) of the protein backbone atoms agree with molecular dynamics simulation. Below 180 K the MSFs of the heme iron agree with the data from Mössbauer spectroscopy. The MSFs of the iron atom relative to the heme are an order of magnitude smaller than the total MSFs of the iron atom. They agree with the data from optical absorption spectroscopy. Thus the MSFs of the iron atom as measured by Mössbauer spectroscopy can be used to probe the overall motion of the heme within the protein matrix, whereas the Gaussian thermal line broadening of the Soret band and the resonance Raman bands can be used to detect local intramolecular iron-porphyrin motions.

INTRODUCTION

At low temperatures many aspects of the dynamic behavior of protein-water systems are similar to other, more conventional solids like crystals of small organic molecules or glasses (Frauenfelder et al., 1988, 1991; Parak and Nienhaus, 1991; Nienhaus and Parak, 1994). This is also valid for the temperature dependence of the mean square fluctuation (MSF) of protein atoms, which below 180 K increases linearly with temperature. The temperature dependence suggests that harmonic modes of motion are responsible for the flexibility. At higher temperatures strong anharmonicities become evident. They give rise to a nonlinear increase of the MSFs of protein atoms, which can be observed above 180 K. This additional flexibility is typical for protein molecules, but also for glasses. It can, for instance, be measured by RSMR or Mössbauer spectroscopy (Parak, 1985; Frauenfelder et al., 1988). The latter is only possible for iron-containing proteins like myoglobin. For proteins containing heme as a cofactor, the line broadening of the Soret band can also be used to derive the MSF of the iron atom relative to the porphyrin (Leone et al., 1994). The position and isotope shift of the resonance Raman band of myoglobin (Mb) at 222 cm^{-1} (Argade et al., 1984; Gilch et al., 1995) depend on the elastic constants of the harmonic potential binding the iron atom to the nitrogen atoms of the porphyrin and the imidazole ring of the proximal histidine 93.

The MSFs of protein atoms can be calculated by computer simulation of the dynamics. However, as long as the motion of the atoms can be described in the harmonic approximation, which should be the case at low temperature, a normal-mode analysis can be more suitable. Recent reviews of the normal-mode formalism are given by Case (1994) and Janezic and Brooks (1995). In the present paper the MSFs of deoxymyoglobin (Mb) and CO-ligated myoglobin (MbCO) averaged over all protein backbone atoms and the MSF of the iron atom are calculated in the harmonic approximation. The MSFs derived from computer simulations of the molecular dynamics can be compared with experimental data from Mössbauer absorption of the iron nucleus and from optical absorption spectroscopy of the Soret band. The amplitude of the motion of the iron atom perpendicular to the heme plane depends critically on the force constants of the iron porphyrin and imidazole nitrogen bonds. Their values are probed by comparing the measured shift of the Raman band at 222 cm^{-1} from Mb containing ^{54}Fe and ^{57}Fe isotopes in the heme with the corresponding spectra calculated from normal mode analysis. Related normal-mode analyses of Mb without quantitative comparisons with experimental data were performed by Bialek and Goldstein (1985) and Seno and Go (1990).

METHODS

Normal mode formalism

The normal-mode analysis of MbCO is performed for the MbCO crystal structure, which also includes the coordinates of 170 water molecules. The normal modes of Mb are calculated from a structure obtained by removing the CO ligand from the MbCO crystal structure and a subsequent energy minimization of the resulting structure. Polar hydrogen atoms are added with CHARMM (Brooks et al., 1983). Nonpolar hydrogen atoms are represented by corresponding extended-type carbon atoms. The starting point of the nor-

Received for publication 1 December 1995 and in final form 6 February 1996.

Address reprint requests to Dr. Ernst Walter Knapp, Institut für Kristallographie, Takustraße 6, D-14195 Berlin, Germany. Tel.: 49-30-8384387; Fax: 49-30-8383464; E-mail: knapp@chemie.fu-berlin.de.

0006-3495/96/05/2092/08 $2.00

mal mode analysis is an energy-minimized structure. The energy minimization is performed with the CHARMM force field, using switch cutoff conditions for Lennard-Jones and shift cutoff conditions for Coulomb interactions. The cutoff distance for both interaction types is 8.5 Å. The TIP3P water model (Jorgensen et al., 1983), enhanced by flexible bond lengths and bond angle, is used. The energy parameters for the heme are taken from Kuczera et al. (1990). The atomic partial charges of the heme are adapted from an INDO-CI calculation of the heme, where the Fe^{2+} ion was replaced by a Mg^{2+} ion (Scherer and Fischer, 1989). The myoglobin-water system is considered in isolation, i.e., no constraints like periodic boundary conditions or containment potentials are used. In the first step of energy minimization the heavy atoms are kept fixed, and only the positions of the hydrogen atoms are minimized, with 2200 steps of steepest descent and 400 steps of conjugated gradient method. The energy minimization is continued with 3000 steps of steepest descent and 18,000 steps of conjugated gradient method, where now all atoms are allowed to move. From the energy-minimized structure the Hesse matrix of the Cartesian second-order partial derivatives is evaluated using the CHARMM energy function. The elements of the symmetric Hesse matrix read

$$(\Omega^2)_{ij} = \frac{\partial^2 V(\vec{q})}{\partial q_i \, \partial q_j}, \qquad i,j = 1,2,\ldots 3n. \tag{1}$$

The vector in the argument of the energy function $V(\vec{q})$

$$\vec{q} = (\vec{q}_1, \ldots \vec{q}_n), \tag{2}$$

contains the mass-weighted Cartesian coordinates of the n atoms of the protein-water system. For atom i the mass-weighted three-component $\vec{q}_i$ and normal Cartesian $\vec{r}_i$ coordinate vectors are related as follows:

$$\vec{q}_i = \sqrt{m_i}\vec{r}_i \qquad i = 1,2,\ldots n. \tag{3}$$

The q_i, q_j in the denominator of Eq. 1 denote any of the $N = 3n$ components of the N-component coordinate vector $\vec{q}$ (Eq. 2).

For the considered MbCO-water system containing $n = 2077$ atoms the Hesse matrix has the dimension (6231×6231). In single precision symmetric storage mode the Hesse matrix occupies 155 megabytes of memory. The Hesse matrix is diagonalized by using in a first step the Householder method to obtain a tridiagonal matrix. The eigenvalues ω_i^2 of this matrix are then calculated by an Eispack subroutine (Garbow et al., 1977) using the implicit QL method and stored in ascending order, i.e., $\omega_i^2 < \omega_{i+1}^2$. Finally, each dimensionless eigenvector $\vec{d}^k$ is evaluated separately by solving the N-dimensional homogeneous linear equation systems for the corresponding eigenvalue ω_k^2:

$$(\Omega^2 - \omega_k^2 \mathbf{1}) \circ \vec{d}^k = \vec{0}, \qquad k = 1,2\ldots N, \tag{4}$$

where $\mathbf{1}$ is the $(N \times N)$ unit matrix and $\vec{0}$ is a vector whose $N = 3n$ components vanish.

For an energy-minimized structure of a molecule the Hesse matrix is positive semi-definite. As a consequence the eigenvalues ω_k^2 of the Hesse matrix are greater than or equal to zero. For a three-dimensional molecule in isolation that does not interact with other molecules or an external potential, one obtains six vanishing eigenvalues corresponding to the six degrees of freedom for free rotation and translation. If the energy minimization is not completed, the six lowest eigenvalues of the Hesse matrix do not vanish and can even adopt negative values. Negative eigenvalues are indicative of structural instabilities, which can be healed by energy minimization. Hence these lowest eigenvalues can be used as a quality control for the energy minimization and the diagonalization procedure.

Analysis tools for normal modes

In analogy to the $3n$-dimensional position vector $\vec{q}$ the $3n$-component eigenvector

$$\vec{d}^k = (\vec{d}_1^k, \vec{d}_2^k, \ldots \vec{d}_n^k) \tag{5}$$

can be decomposed to n three-component vectors:

$$\vec{d}_i^k = (d_{i1}^k, d_{i2}^k, d_{i3}^k), \tag{6}$$

where d_{ij}^k is the jth normalized Cartesian component of atom i in the eigenvector of the kth normal mode. The resulting MSF of atom i with respect to normal mode k can be written as

$$\langle(\vec{r}_i^k)^2\rangle = (\vec{d}_i^k)^2[\sigma_i^k(T)]^2, \qquad k = 1,2\ldots N, \quad i = 1,2\ldots n. \tag{7}$$

The square of an amplitude of fluctuation of atom i with respect to normal mode k, $(\sigma_i^k)^2$, can be expressed as

$$[\sigma_{i,\mathrm{class}}^k(T)]^2 = \frac{k_B T}{m_i \omega_k^2}; \quad [\sigma_{i,\mathrm{qm}}^k(T)]^2 = \frac{\hbar}{2m_i\omega_k} coth\left(\frac{\hbar\omega_k}{2k_B T}\right) \tag{8}$$

for classical and quantum mechanics, respectively. Note that the $3n$ component eigenvectors (Eq. 5) are normalized to unity, $\vec{d}^k \circ \vec{d}^k = 1$.

At vanishing temperature the square of the quantum mechanical amplitude simplifies to the expression

$$[\sigma_{i,\mathrm{qm}}^k(0)]^2 = \frac{\hbar}{2m_i\omega_k}. \tag{9}$$

At high temperatures the quantum mechanical expression in Eq. 8 merges with the classical expression.

The total MSF of atom i due to all normal modes with the exception of the diverging contribution from the six zero frequency modes of free translation and rotation is given by

$$\langle\vec{r}_i^2\rangle = \sum_{k=7}^{3n} \langle(\vec{r}_i^k)^2\rangle. \tag{10}$$

The MSF of atom i in the spatial direction of unit vector $\vec{s}$ is given by

$$\langle(\vec{r}_i \circ \vec{s})^2\rangle = \sum_{k=7}^{3n} (\vec{d}_i^{\,k} \circ \vec{s})^2 \cdot (\sigma_i^k(T))^2. \quad (11)$$

The MSF of the iron atom relative to the center of mass of the carbon atom skeleton of the heme

$$\vec{r}_c = \frac{1}{20}\sum_{i=1}^{20} \vec{r}_{c_i}, \quad (12)$$

involving 20 carbon atoms can be expressed as

$$\langle \vec{r}_{Fe}{}^2\rangle_{heme} = \langle(\vec{r}_{Fe} - \vec{r}_c)^2\rangle \quad (13)$$

$$= \sum_k [\sigma_{Fe}^k(T)\vec{d}_{Fe}^{\,k} - \sigma_C^k(T)\frac{1}{20}\sum_{i=1}^{20}\vec{d}_{C_i}^{\,k}]^2,$$

where σ_{Fe} and σ_C contain the masses of the iron and carbon atoms, respectively. In analogy to Eqs. 7 and 11 the out-of-plane contributions of the MSF of the iron atom relative to the porphyrin carbon atom skeleton are given by

$$\langle \vec{r}_{Fe,\perp}{}^2\rangle_{heme} = \langle[(\vec{r}_{Fe} - \vec{r}_C) \circ \vec{s}]^2\rangle \quad (14)$$

$$= \sum_k [\sigma_{Fe}^k(T)\vec{s} \circ \vec{d}_{Fe}^{\,k} - \sigma_C^k(T)\frac{1}{20}\sum_{i=1}^{20}\vec{s} \circ \vec{d}_{C_i}^{\,k}]^2.$$

Here $\vec{s}$ is the unit three-component vector perpendicular to the heme plane, defined by the carbon atom skeleton.

The in-plane contributions of the MSFs of the iron atom relative to the center of mass of the carbon atoms of the heme can be calculated by subtracting the out-of-plane contribution from the corresponding total MSF:

$$\langle \vec{r}^2_{Fe,II}\rangle_{heme} = \langle \vec{r}^2_{Fe}\rangle_{heme} - \langle \vec{r}^2_{Fe,\perp}\rangle_{heme}. \quad (15)$$

The spectrum of Raman scattering intensity can be expressed by

$$I_R(\omega) = \sum_{k=7}^{N} \alpha_k^2\, \delta(\omega - \omega_k), \quad (16)$$

where α_k is the polarizability of the molecular system with respect to the kth eigenmode at frequency ω_k. If the excitation energy is in resonance with an electronic excited state, the polarization is strongly influenced by the energy denominator (Lee and Heller, 1979). The measured shift of the resonance Raman spectrum for Mb with the isotopes ^{54}Fe and ^{57}Fe can be used to probe the force constants of the iron atom with the porphyrin and imidazole nitrogen atoms used in the CHARMM energy function for the heme (Kuczera et al., 1990). It is known that the vibrational mode, which is active in the resonance Raman spectrum of Mb and sensitive to the isotopic effect, is an iron out-of-plane motion, where the imidazole nitrogen atom of histidine 93 moves in a direction opposite that of the iron atom movement (Argade et al., 1984; Gilch et al., 1995).

Because the polarizability tensors for the vibrational modes of the heme are not readily available, a projection technique is used that filters the iron out-of-plane motion out of all vibrational modes. The corresponding projection is defined by the $3n$-dimensional unit vector

$$\vec{P}_R = (\vec{p}_1, \vec{p}_2, \ldots \vec{p}_n). \quad (17)$$

To pick up contributions of the iron as well as porphyrin and imidazole nitrogen atoms, all components of $\vec{p}_R$ vanish, except the three-component vectors $\vec{p}_i$ referring to the iron atom

$$\vec{p}_{Fe} = \vec{s}\sqrt{\frac{\mu}{m_{Fe}}} \quad (18)$$

and to each of the four porphyrin and the one imidazole nitrogen atoms of the proximal histidine

$$\vec{p}_{N_i} = -\frac{\vec{s}}{5}\cdot\sqrt{\frac{\mu}{m_N}} \qquad i = 1, 2, 3, 4, 5. \quad (19)$$

In Eqs. 18 and 19 m_{Fe} and m_N are the masses of the iron and nitrogen atoms and μ is the reduced mass:

$$\mu = \frac{5m_N m_{Fe}}{5m_N + m_{Fe}}. \quad (20)$$

Note that $\vec{p}_R$ refers to mass-weighted coordinates in the center of mass system of the six considered atoms. The motion of the atoms perpendicular to the heme plane occurs along the unit-length three-component normal vector $\vec{s}$. The heme plane is defined as the average over the 20 carbon atoms of the porphyrin. With this filter device the resonance Raman scattering intensity of the iron out-of-plane motion can be qualitatively expressed by

$$I_R(\omega) = \sum_{k=7}^{N} (\vec{d}^{\,k} \circ \vec{p}_R)^2 \cdot \delta(\omega - \omega_k). \quad (21)$$

For applications the delta function in Eq. 21 is replaced by a suitable Gaussian lineshape function.

Analysis of the broadening of the Soret band

A considerable fraction of the variance of the Gaussian lineshape σ^2_{opt} of the Soret band arises from line broadening due to the coupling of the electronic transition with a bath of low-frequency modes (Schomacker and Champion, 1986; Srajer et al., 1986; Srajer and Champion, 1991; Di Pace et al., 1992). In previous work (Di Pace et al., 1992; Cupane et al., 1993, 1995; Leone et al., 1994) the bath of low-frequency modes with $\omega_k < 500\ cm^{-1}$ was treated as a set of N degenerate, uncoupled, quantum mechanical, harmonic Einstein oscillators of frequency $\langle\omega\rangle$. Vibrational modes of higher frequency appear in vibronic bands, which are sep-

arated from the main Soret band (Cupane et al., 1995). Therefore, they do not contribute to the line broadening of the Soret band. With this assumption the temperature dependence of the variance of the Gaussian-shaped Soret band reads

$$\sigma^2_{\mathrm{opt}}(T) = \frac{NS}{(2\pi)^2}\langle\omega\rangle^2 \coth\left(\frac{\hbar\langle\omega\rangle}{2k_BT}\right) + \sigma^2_{\mathrm{inhom}}. \quad (22)$$

S is the linear coupling constant of each Einstein oscillator with the electronic transition, and the term $\sigma^2_{\mathrm{inhom}}$ is due to other inhomogeneous broadening mechanisms.

In the present approach a cruder approximation is used, where a single Einstein oscillator with the mass of the iron atom is considered. It describes the motion of the iron atom relative to the heme skeleton. The quantum mechanical mean square displacement of the motion of the iron atom relative to the heme can then be represented by (see also Eq. 8)

$$\langle\vec{r}^2_{\mathrm{Fe}}\rangle = \frac{\hbar}{2m_{\mathrm{Fe}}\langle\omega\rangle}\coth\left(\frac{\hbar\langle\omega\rangle}{2k_BT}\right). \quad (23)$$

Finally, from Eqs. 22 and 23 it follows that the MSFs of the iron atom relative to the heme derived from the Gaussian bandwidth of the Soret band can be written as

$$\langle\vec{r}^2_{\mathrm{Fe}}\rangle_{\mathrm{opt}} = \frac{\hbar}{2m_{\mathrm{Fe}}\langle\omega\rangle}(2\pi)^2\frac{\sigma^2_{\mathrm{opt}}(t) - \sigma^2_{\mathrm{inhom}}}{NS\langle\omega\rangle^2}. \quad (24)$$

RESULTS AND DISCUSSION

Vibrational motions from normal mode analysis

The root mean square deviation (RMSD) of the energy-minimized structure and crystal structure of MbCO averaged over the protein backbone atoms (C, C_α, N) amounts to 0.926 Å. This is a RMSD value typical of energy-minimized protein structures. The seven lowest eigenvalues of the normal mode analysis are $\omega_1^2 = -5.2 \times 10^{-5}\ \mathrm{cm}^{-2}$, $\omega_2^2 = -1.5 \times 10^{-8}\ \mathrm{cm}^{-2}$, $\omega_3^2 = -4.4 \times 10^{-10}\ \mathrm{cm}^{-2}$, $\omega_4^2 = -1.8 \times 10^{-10}\ \mathrm{cm}^{-2}$, $\omega_5^2 = 5.8 \times 10^{-5}\ \mathrm{cm}^{-2}$, $\omega_6^2 = 7.5 \times 10^{-5}\ \mathrm{cm}^{-2}$, and $\omega_7^2 = 52.4\ \mathrm{cm}^{-2}$. The six lowest eigenvalues corresponding to free rotation and translation of the whole protein-water system are very close to zero, indicating that the energy minimization is converged and the diagonalization of the Hesse matrix is performed properly. The lowest nonvanishing eigenvalue ω_7^2 is well separated from the first six vanishing eigenvalues. From an inspection of the normal modes it follows that this low-frequency mode is dominated by motions of secondary structure motifs. A considerable fraction of low-frequency modes up to a frequency of 30 cm^{-1} are of this type. These vibrational modes contribute significantly to the MSFs of protein backbone atoms. In the absence of water molecules the lowest nonvanishing eigenvalue is larger ($\omega_7^2 = 162.4$). Nevertheless, the sum of MSFs of protein backbone atoms from all normal modes is larger in the absence of water. From this one can conclude that water molecules are on the average constraining the mobility of protein atoms.

The spectrum of frequencies ω_i of equal intensity, i.e., the density of state (DOS) spectrum, from a normal mode analysis of the MbCO water system is depicted in Fig. 1. For the individual components a Gaussian lineshape with a full width at half-height (FWHH) of 8.5 cm^{-1} is used to smooth the DOS spectrum. The DOS spectrum extends from the lowest frequency at 7.2 cm^{-1} up to frequencies of 3648 cm^{-1}, which correspond to bond-stretching modes of hydrogen atoms. There are nine normal modes whose frequencies are below 12.0 cm^{-1}. Seno and Go (1990) obtained for this case only six normal modes, presumably because they considered Mb without water molecules. These nine modes contribute 28% to the total MSF of the iron atom in MbCO calculated by normal-mode analysis. The normal-mode analysis from Seno and Go (1990) reveals that 57% of the conformational change between Mb and MbO_2 can be accounted for by the six normal modes of lowest frequency.

In principle one can discriminate three different contributions to the MSFs of the iron atoms: i) an intermolecular component due to the motion of myoglobin molecules relative to each other; ii) an intramolecular contribution involving the motion of the whole heme group together with the iron atom and perhaps some globin parts as the HIS F8 relative to the globin moiety; iii) an intramolecular contribution that is due to the motion of the iron atom relative to the atoms of the heme. The first contribution is formally contained in the first six vanishing eigenvalues ($\omega_i^2 = 0$). It is shown in Eqs. 17–21 how one can filter out the contributions of iii) from the results of normal-mode analysis.

Resonance Raman intensities of myoglobin

The ratio of motion of the heme as a whole versus the intramolecular vibration of the iron atom relative to the heme sensed by the iron atom depends critically on the binding strength of the iron atom with the porphyrin and imidazole nitrogen atoms. The correct value of the corresponding elastic constants can be

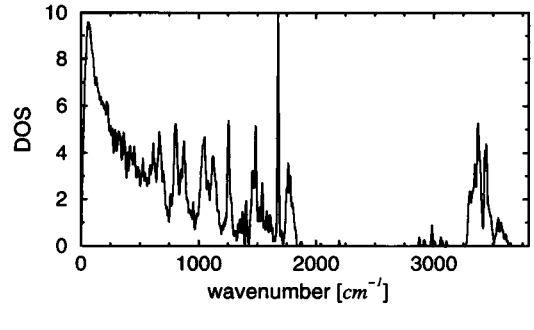

FIGURE 1 Calculated vibrational density of state spectrum (DOS) of MbCO with 170 crystal water molecules. The amide I band is represented by the peak at 1680 cm^{-1}. The broad peak at 1800 cm^{-1} is due to the 170 crystal water molecules. The DOS spectrum shows significant contributions from vibrational modes of crystal water and should not be directly compared with a dry MbCO spectrum.

probed by relating the out-of-plane vibration of the iron atom with resonance Raman spectra. For this purpose the vibrational frequencies and the isotopic shift of the resonance Raman scattering intensities (Argade et al., 1984) are compared with the results from a normal-mode analysis of Mb.

In Fig. 2 the resonance Raman scattering intensities of Mb are compared with calculated vibrational spectra of Mb, where the intensities are obtained according to Eq. 21 using a projection (Eqs. 17–19) that picks out the iron out-of-plane modes. The displayed frequency range involves the iron out-of-plane vibrational modes with the lowest frequencies that carry significant intensity. The calculated peak frequency of about 232 cm^{-1} is 10 cm^{-1} higher than the experimental value of 222 cm^{-1}. To facilitate a comparison between theory and experiment the calculated Raman spectrum is red-shifted by 10 cm^{-1}. The vibrational bands are represented by Gaussian lineshapes of equal width, whose value of 16 cm^{-1} (FWHH) is optimized to fit the shape of the experimental Raman band (Fig. 2 *A*). The intensity of the calculated spectrum is adjusted to the measured resonance Raman spectra of Mb only for the isotope ^{57}Fe. The same scale factor is used for the calculated Raman spectrum with ^{54}Fe and Raman difference spectrum (Fig. 2 *B*). The calculated isotopic shift increases with the assumed value of the Gaussian linewidth. For the optimized linewidth the calculated isotopic shift referring to Mb amounts to 2.1 cm^{-1}, as compared to a measured isotopic shift of 1.5 cm^{-1} (Argade et al., 1984).

The agreement of the calculated spectrum with the measured resonance Raman spectrum is not very sensitive to details of the projection (Eqs. 17–21). From the agreement of the calculated and measured resonance Raman scattering intensities one can conclude that the force constants for binding of the iron atom to the porphyrin and imidazole nitrogen atoms used in the energy function have reasonable values.

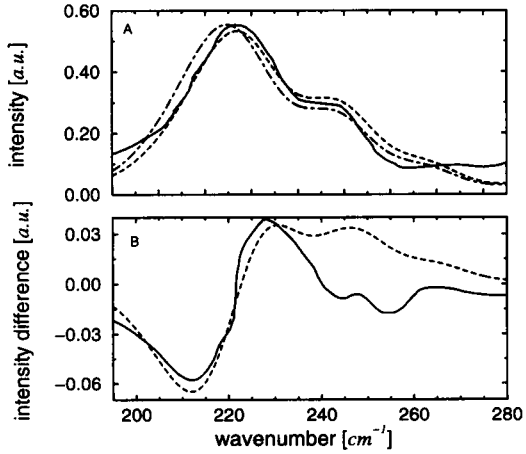

FIGURE 2 (*A*) Resonance Raman spectrum of deoxymyoglobin. Experimental data of Mb with ^{54}Fe (Argade et al., 1984) (——); spectrum calculated according to Eq. 21 from normal mode analysis of the Mb-water system with ^{54}Fe (– – –) and ^{57}Fe (–·–·–). (*B*) Difference Raman spectrum of Mb (^{54}Fe minus ^{57}Fe). ——, Experimental data of Mb (Argade et al., 1984); – – –, normal mode analysis of the Mb-water system. To facilitate a comparison between theory and experiment the calculated spectra are red-shifted by 10 cm^{-1}.

Total fluctuations of the heme iron atom

The low-temperature MSFs of the MbCO atoms depicted in Fig. 3 are calculated from the results of normal-mode analysis according to Eqs. 7 and 8, classical case, using the CHARMM force field. The MSFs of the protein atoms are calculated from the normal-mode analysis of MbCO with 170 crystal water molecules, as described in the section on analysis tools for normal modes. For the sake of clarity, quantum mechanical contributions to the low-temperature dependence of the MSFs that are due to zero point oscillations are ignored. They lead to a nonlinear temperature dependence of the MSFs at very low temperatures and result in nonvanishing albeit small MSFs at zero temperature. However, small anharmonicities are also present at low temperatures and act as a friction mechanism on the vibrational modes. In the presence of friction, quantum corrections due to zero point oscillations diminish (Caldeira and Leggett, 1983). At temperatures above 50 K the quantum mechanical version of the temperature dependence of the MSF becomes linear and merges with the classical mechanics approximation. This is valid for the total MSF of the iron atom, which is dominated by low-frequency modes where large parts of the protein molecule move cooperatively. The intramolecular iron-heme vibrations are at higher frequencies and are more localized. As a consequence the classical linear behavior of the MSF sets in at higher temperatures (see Fig. 4). Fur-

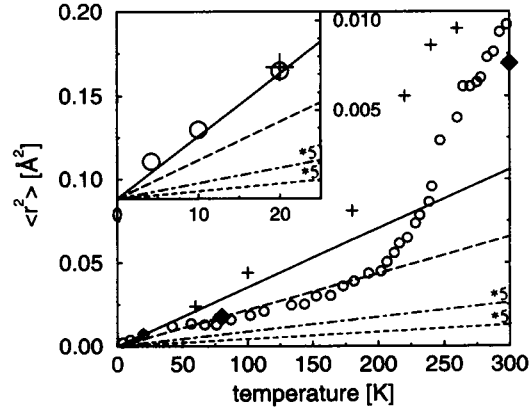

FIGURE 3 Mean square fluctuations of myoglobin (Mb, MbCO). ○, Iron atom fluctuations of Mb from Mössbauer spectroscopy (Parak et al., 1982); +, fluctuations of protein backbone atoms (N-C_α-C) from molecular dynamics simulation of MbCO with 350 water molecules (Loncharich and Brooks, 1990); ◆, iron fluctuations from molecular dynamics of MbCO in vacuum (Kuczera et al., 1990) at 80 and 325 K. To include the high-temperature data point it was placed at 300 K. The linear plots are results from normal mode analysis of MbCO with 170 crystal water molecules using the temperature dependence according to classical mechanics (Eq. 8). ——, Fluctuations of protein backbone atoms (N-C_α-C); – – –, total iron atom fluctuations; - - - -, iron atom fluctuations perpendicular to the porphyrin carbon atom skeleton, enlarged by a factor of 5; –·–·–, iron atom fluctuations relative to the center of mass of the porphyrin carbon atom skeleton, enlarged by a factor of 5.

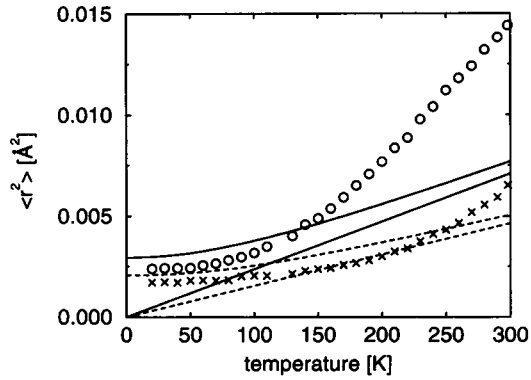

FIGURE 4 Comparison of low frequency ($\omega_k < 500\ cm^{-1}$) MSFs of the iron atom relative to the porphyrin carbon atom skeleton MSFs derived from normal mode analysis (——, Mb; – – –, MbCO) and the line broadening of the Soret band absorption (○, Mb; ×, MbCO). The classical (vanishing at zero temperature) and the quantum mechanical version of the MSF calculated from normal mode analysis are displayed. Only the low-frequency portion of the MSFs of the iron atom can be compared with the Soret band broadening, as explained in the section on analysis of the broadening of the Soret band.

thermore, localized vibrational modes of higher frequency are less influenced by friction mechanisms. Hence in this case quantum corrections remain important. Therefore in Fig. 4 the iron atom MSF relative to the heme is displayed with the quantum corrections that are due to the zero point oscillations.

At low temperatures (20 K) the calculated MSFs averaged over all backbone atoms (Fig. 3, *solid line*) agree well with corresponding molecular dynamics (MD) simulation data of MbCO with 349 water molecules (Loncharich and Brooks, 1990; Steinbach et al., 1991) (see + in *inset* of Fig. 3). However, already at 100 K the protein backbone fluctuations from MD data exhibit small anharmonic contributions, which become significant above 200 K. At 80 K and 325 K MD data of the iron atom fluctuation of MbCO in vacuum are available (Kuczera et al., 1990, see the *filled diamond* in Fig. 3). The low temperature point of MSF from the MD simulation agrees quantitatively with the normal-mode result. At 325 K the iron fluctuation reveals strong anharmonicities. No data at intermediate temperatures are available. In spite of the short simulation time of 120 ps, the calculated MSFs of the iron atom are close to the values obtained from Mössbauer spectroscopy, where the MSFs are sampled for 10^5 ps. This puzzle was pointed out before (Parak and Knapp, 1984). The two data points of iron fluctuations obtained from MD simulations of MbCO in vacuum at 80 K and 325 K are not sufficient to decide whether the anharmonicities of the iron fluctuations appear at the same temperature as in the data from the Mössbauer spectra. Below 200 K the MSF of the iron atom calculated by normal-mode analysis (*long-dashed line* in Fig. 3) using Eq. 8 agrees well with the MSF derived from the Lamb-Mössbauer factor (Parak, 1985). From the Mössbauer spectrum below 200 K one can conclude that the fluctuations of the iron atom in MbCO behave less anharmonically than the fluctuation of the protein backbone as derived from MD simulations.

The contributions of the intramolecular vibrational modes of the iron atom relative to the heme are also displayed in Fig. 3 (enlarged by a factor of 5, *dashed-dotted line*). The out-of-plane MSFs of the iron atom relative to the carbon atom skeleton of the heme $\langle \vec{r}^2_{Fe,\perp} \rangle_{heme}$ are evaluated according to Eq. 14 and plotted in Fig. 3 (*short dashed line*). The in-plane contributions of the MSFs of the iron atom are only slightly larger than the out-of-plane contributions. Thus the total MSFs of the iron atom relative to the center of mass of the carbon atom skeleton of the heme are about twice as large as the out-of-plane contribution (*dashed-dotted line*). The MSFs of the iron atom relative to the center of mass of the carbon atoms of the heme also involve contributions from intra-heme vibrational modes where the porphyrin nitrogen atoms oscillate in phase with the iron atom. Therefore, the MSFs of the iron atom relative to the center of mass of the four porphyrin nitrogen atoms is about 1.8 times smaller than the corresponding MSFs relative to the center of mass of the carbon atoms of the heme. The intra-heme vibrational contribution to the MSFs of the iron atom referring to the carbon atom skeleton is only about 13% of the total MSF of the iron atom (*long-dashed line* in Fig. 3). Therefore, the total MSFs at the iron atom measured by Mössbauer spectroscopy probe the protein-specific fluctuations rather than the intra-heme vibrations of the iron atom.

Fluctuations of the iron atom with respect to heme

The vibronic band of the high-frequency modes is separated from the Soret band and therefore does not contribute to the Soret band broadening (Cupane et al., 1995). Hence in Fig. 4 only the low-frequency ($\omega_k < 500\ cm^{-1}$) MSFs of the iron atom with respect to the center of mass of the heme obtained from normal-mode analysis are compared with those obtained from optical absorption spectroscopy using Eq. 24. The local intra-heme vibrational modes have higher frequencies and are more localized than those that provide the major contribution to the total MSFs of the iron atom. Therefore, they have a larger relative contribution from zero point oscillations. The damping of these vibrational modes relative to their frequency value is usually less than that of low-frequency modes. Hence quantum corrections are more important here. The values of $\sigma^2_{opt}(T)$, σ^2_{inhom}, NS, and $\langle\omega\rangle$ are taken from Cupane et al. (1995). The wave functions involved in the transition $\pi \rightarrow \pi^*$ giving rise to the Soret band absorption are delocalized over the whole porphyrin plane. Therefore, it is appropriate to compare $\langle \vec{r}^2_{Fe} \rangle_{opt}$ with the MSFs of the iron atom relative to the center of mass of the carbon atoms of the heme $\langle \vec{r}^2_{Fe} \rangle_{heme}$ rather than relative to the four porphyrin nitrogen atoms only. In Eq. 13 of $\langle \vec{r}^2_{Fe} \rangle_{heme}$ the sum over vibrational modes runs from $k = 7$ to $\max_k$ (k, with $\omega_k < 500\ cm^{-1}$) to account for the low-frequency modes only. In Mb the high-frequency modes ($\omega_k \geq 500\ cm^{-1}$) contribute essentially a constant value of 0.0005 Å^2 to the MSF of the iron atom.

The classical and quantum mechanical results of the MSFs obtained from the normal-mode analysis and from the

optical absorption spectra show that the MSFs of the iron atom relative to the heme are larger in Mb than in MbCO (Fig. 4). One can argue that the dominant contributions of the MSFs of the iron atom relative to the heme in MbCO are due to vibrational modes, where the iron atom moves in phase with the CO ligand. Hence these modes should have larger reduced masses in MbCO than in Mb. From this fact one can naively conclude that the difference in the MSF of Mb and MbCO can be explained by the mass dependence inherent in the expression of the MSF, which in the classical limit is inversely proportional to $m\omega^2$. However, because $k = m\omega^2$ is the force constant of the corresponding harmonic restoring potential, $m\omega^2$ is mass independent. Therefore, in the classical limit this argument does not hold. A more suitable explanation is that in Mb the iron atom can move more freely than in MbCO, where the ligand occupies the heme pocket and thus constraints the motion of the iron atom. This would effectively correspond to an increase in the force constant k.

The quantum mechanical version of the MSF exhibits an explicit dependence on the mass and the force constant, which at vanishing temperatures is inversely proportional to $\sqrt{m \cdot k}$ (Eq. 9). Although the dependence on the force constant is weaker for the quantum mechanical than for the classical MSF, the additional mass dependence of the quantum mechanical MSF should yield a relative difference of the MSF from Mb and MbCO, which at low temperatures is as large as in the classical limit. However, the calculated relative difference of the MSFs between Mb and MbCO is smaller at low temperatures than at room temperature and can be explained by the dependence on the force constant alone. At low temperatures the difference of the MSFs between Mb and MbCO obtained from absorption spectroscopy agrees with the results from normal-mode analysis. Because of the dominant contributions from high-frequency vibrational modes, even at room temperature the quantum mechanical values of the MSFs have not yet reached the classical limit.

At low temperatures $\langle \vec{r}^2_{Fe} \rangle_{opt}$ for Mb and MbCO obtained from optical spectroscopy agrees with the MSFs of the iron atom relative to the heme calculated from normal-mode analysis (Fig. 4). Both $\langle \vec{r}^2_{Fe} \rangle_{opt}$ and the iron-heme MSFs calculated from normal mode analysis are much smaller than the iron fluctuations measured with Mössbauer spectroscopy. Note the order of magnitude difference in the ordinate scales of Figs. 3 and 4. This confirms that Mössbauer spectroscopy probes fluctuations of larger parts of the protein rather than the intra-heme vibrations only.

The anharmonic contributions of the iron atom motions in MbCO obtained from optical and Mössbauer spectroscopy (Di Pace et al., 1992; Parak et al., 1982) appear at the same temperature (180 K). This implies that the motions of the iron atom relative to the heme are also coupled to protein-specific fluctuations, likely through the iron-proximal histidine bond. In Mb the anharmonic contributions from optical absorption spectra appear already above 120 K. This may be due to the larger flexibility of the iron atom available when the heme pocket is not occupied by a CO ligand. As compared to the total MSFs of the iron atom, these intra-heme fluctuations are so small that in the temperature regime between 120 K and 180 K they can hardly be detected by Mössbauer spectroscopy.

CONCLUSIONS

The protein dynamics of myoglobin has been investigated by many experimental techniques. It is especially important to compare the different results to come to a unique physical description. Moreover, it is important to give a theoretical description of the dynamical processes. This paper shows that a normal-mode analysis can explain the mean square displacements of the iron atom in myoglobin at low temperatures obtained from Mössbauer spectroscopy and derived from the Gaussian line broadening of the Soret band.

The Lamb-Mössbauer factor of ^{57}Fe is sensitive to all contributions of the MSFs of the iron atom relative to the laboratory frame occurring on a time scale faster than 100 ns. To explain the MSFs below 180 K one has to consider in particular all normal modes where the iron atom moves in phase with the atoms of the heme group. Normal modes, which contribute only to the motion of the iron atom relative to the heme group, yield MSFs that are much to small.

Acoustic phonon modes can be characterized by motions in which equivalent atoms in several neighbor molecules move in phase. In a single molecule approximation these acoustic phonon modes degenerate to the three free translations. Together with the three free rotations of the protein molecule they constitute the six vibrational modes of zero frequency. These zero frequency modes, of course, cannot be used in a comparison with the MSFs obtained from Mössbauer spectroscopy. However, because the motion of the heme group relative to the protein moiety is sufficient for an explanation of the MSFs from Mössbauer spectroscopy, it is obvious that acoustic phonon modes cannot play an important role. This seems plausible. For a solid with L identical molecules, each containing N atoms, there are only $3L$ acoustic phonon modes, as compared to $(N - 1)3L - 6$ optical and local intramolecular modes. Hence, in a solid composed of macromolecules the influence of acoustic phonon modes on the magnitude of MFSs should also be small. This is in contrast to the work of Bialek and Goldstein (1985), which assumed that acoustic phonons provide the dominant contribution to the MSFs of the iron atom in Mb, thus explaining the MSFs measured by Mössbauer spectroscopy. It must be emphasized that the normal-mode analysis of a single protein molecule does not allow us to discriminate between local intramolecular modes and optical phonons with long-range correlation. Hence from the present study one cannot decide whether the major part of the MSFs at the iron atom in Mb is due to local or optical vibrational modes.

The MSFs of the iron atom relative to the heme in Mb and MbCO as derived from the Gaussian line broadening of

the Soret band agree well with the MSFs of the iron atom with respect to the center of mass of the heme calculated from the normal-mode analysis. This confirms a suggestion by Leone et al. (1994) that optical spectroscopy essentially probes motions of the iron atom with respect to the porphyrin carbon atom skeleton. These motions are more than one order of magnitude smaller than those probed by Mössbauer spectroscopy. Optical spectroscopy therefore appears to be a fine probe of local iron-heme vibrations. In agreement with results from normal-mode analysis, the experimental data in Fig. 4 show that these local motions depend upon the ligation state of Mb, in contrast to Mössbauer spectroscopy. The total MSF of the iron atom derived from normal-mode analysis is also insensitive to the ligation state of Mb. This is not surprising, because the major part of the total MSF of the iron atom in Mb is due to vibrational modes in which the heme and its protein neighborhood move in phase. Thus in these vibrations the CO ligand encounters no strong interactions with the protein moiety.

The shape and isotopic shift of the measured resonance Raman active bands of Mb at 222 cm^{-1} correlate well with results from normal-mode analysis. This agreement depends critically on the energy parameters used for the interactions of the iron atom of the heme with the porphyrin and imidazole nitrogen atoms. It puts the conclusions drawn from the comparison between normal analysis and Mössbauer and optical absorption spectroscopy on a firmer basis.

Finally, it is gratifying to observe that the low-temperature MSFs calculated from normal mode analysis and MD simulation data agree. Although the same energy function is used for both methods, the normal-mode analysis probes only the local curvature of the energy function for a single conformation in a local energy minimum, whereas the MD simulation method explores a larger neighborhood in the conformational space. Nevertheless, the single energy-minimized conformation is representative of all conformations available in the MD simulation at low temperatures. However, anharmonic contributions to the MSFs obtained by MD simulations seem to set in more gradually and at temperatures much lower than observed in experiments.

The authors thank Wolfgang Dreybrodt and Klaus Achterhold for valuable discussions. The CHARMM source code was provided by Martin Karplus and MSI, Inc.

This work was supported by the Deutsche Forschungsgemeinschaft, SFB 312 Project D7, the Fonds of the Deutsche Chemische Industrie, and the EU-net "The dynamics of protein structure."

REFERENCES

Argade, P. V., M. Sassaroli, and D. L. Rousseau. 1984. Confirmation of the assignment of the iron-histidine stretching mode in myoglobin. *J. Am. Chem. Soc.* 106:6593–6596.

Bialek, W., and R. F. Goldstein. 1985. Do vibrational spectroscopies uniquely describe protein dynamics? *Biophys. J.* 48:1027–1044.

Brooks, B. R., R. E. Bruccoleri, B. D. Olafson, D. J. States, S. Swaminathan, and M. Karplus. 1983. CHARMM: a program for macromolecular energy, minimization, and dynamics calculation. *J. Comp. Chem.* 4:187–217.

Caldeira, A. O., and A. J. Leggett. 1983. Quantum tunneling in a dissipative system. *Ann. Phys.* 149:374–456.

Case, D. A. 1994. Normal mode analysis of protein dynamics. *Curr. Opin. Struct. Biol.* 4:285–290.

Cupane, A., M. Leone, and E. Vitrano. 1993. Protein dynamics: conformational disorder, vibrational coupling and anharmonicity in deoxyhemoglobin and myoglobin. *Eur. Biophys. J.* 21:385–391.

Cupane, A., M. Leone, and E. Vitrano, and L. Cordone. 1995. Low temperature optical absorption spectroscopy: an approach to the study of stereodynamic properties of heme proteins. *Eur. Biophys. J.* 23:385–398.

Di Pace, A., A. Cupane, M. Leone, E. Vitrano, and L. Cordone. 1992. Vibrational coupling, spectral broadening mechanisms and anharmonicity effects in carbonmonoxy heme proteins studied by the temperature dependence of the Soret band lineshape. *Biophys. J.* 63:475–484.

Doster, W., S. Cusack, and W. Petry. 1989. Dynamical transition of myoglobin revealed by inelastic neutron scattering. *Nature.* 337:754–756.

Frauenfelder, H., F. Parak, and R. D. Young. 1988. Conformational substrates in proteins. *Annu. Rev. Biophys. Biophys. Chem.* 17:451–479.

Frauenfelder, H., S. G. Sligar, and P. G. Wolynes. 1991. The energy landscapes and motions of proteins. *Science.* 254:1598–1603.

Garbow, B. S., J. M. Boyle, J. J. Dongarra, and C. B. Moler. 1977. Matrix Eigensystem Routines—EISPACK Guide Extension. Springer, Berlin.

Gilch, H., W. Dreybrodt, and R. Schweitzer-Stenner. 1995. Thermal fluctuations between conformational substrates of the Fe^{2+}-His^{F8} linkage in deoxymyoglobin probed by the Raman active Fe-N_ϵ (His^{F8}) stretching vibration. *Biophys. J.* 69:214–227.

Janezic, D., and B. R. Brooks. 1995. Harmonic analysis of large systems. II. Comparison of different protein models. *J. Comp. Chem.* 16: 1543–1553.

Jorgensen, W. L., J. Chendrasekar, J. Madura, R. Impley, and M. Klein. 1983. Comparison of simple potential functions for simulating liquid water. *J. Chem. Phys.* 79:926–935.

Kuczera, K., J. Kuriyan, and M. Karplus. 1990. Temperature dependence of the structure and dynamics of myoglobin. *J. Mol. Biol.* 213:351–373.

Lee, S.-Y., and E. J. Heller. 1979. Time-dependent theory of Raman scattering. *J. Chem. Phys.* 71:4777–4788.

Leone, M., A. Cupane, V. Militello, and L. Cordone. 1994. Thermal broadening of Soret band in heme complexes and in heme-proteins: role of the iron dynamics. *Eur. Biophys. J.* 23:349–352.

Loncharich, R. J., and B. R. Brooks. 1990. Temperature dependence of dynamics of hydrated myoglobin. Comparison of force field calculations with neutron scattering data. *J. Mol. Biol.* 215:439–455.

Nienhaus, G. U., and F. Parak. 1994. The Mössbauer effect and collective motions in glass-forming liquids and polymeric networks. *Hyperfine Interact.* 90:263–264.

Parak, F. 1985. Strukturfluktuationen in Proteinen. *Phys. Bl.* 41(12):396–400.

Parak, F., and E. W. Knapp. 1984. A consistent picture of protein dynamics. *Proc. Natl. Acad. Sci. USA.* 81:7088–7092.

Parak, F., E. W. Knapp, and D. Kucheida. 1982. Protein dynamics. Mössbauer spectroscopy on deoxymyoglobin crystals. *J. Mol. Biol.* 161: 177–194.

Parak, F., and G. U. Nienhaus. 1991. Glass-like behaviour of proteins as seen by Mössbauer spectroscopy. *J. Non-Crystralline Solids.* 131–133: 362–368.

Scherer, P. O. J., and S. F. Fischer. 1989. Quantum treatment of the optical spectra and the initial electron transfer process within the reaction center of *Rhodopseudomonas viridis. Chem. Phys.* 131:115–127.

Schomacker, K. T., and P. M. Champion. 1986. Investigations of spectral broadening mechanisms in biomolecules: cytochrome *c. J. Chem. Phys.* 84:5314–5325.

Seno, Y., and N. Go. 1990. Deoxymyoglobin studied by the conformational normal mode analysis. II. The conformational change upon oxygenation. *J. Mol. Biol.* 216:111–126.

Srajer, V., and P. M. Champion. 1991. Investigations of optical line shapes and kinetic hole burning in myoglobin. *Biochemistry.* 30:7390–7401.

Srajer, V., K. T. Schomacker, and P. Champion. 1986. Spectral broadening in biomolecules. *Phys. Rev. Lett.* 57:1267–1270.

Steinbach, P. J., R. J. Loncharich, and B. R. Brooks. 1991. The effects of environment and hydration on protein dynamics: a simulation study of myoglobin. *Chem. Phys.* 158:383–394.